CHEMICAL ENGINEERING TRANSACTIONS
VOL. 47, 2016
A publication of AIDIC
The Italian Association of Chemical Engineering
Online at www.aidic.it/cet
Guest Editors: Angelo Chianese, Luca Di Palma, Elisabetta Petrucci, Marco Stoller

ISBN 978-88-95608-38-9; **ISSN** 2283-9216
DOI: 10.3303/CET1647026

Synthesis and Characterization of Copper Ferrite Magnetic Nanoparticles by Hydrothermal Route

Thomas Abo Atia, Pietro Altimari, Emanuela Moscardini, Ida Pettiti, Luigi Toro Francesca Pagnanelli*

Department of Chemistry, Sapienza University of Rome, P.le Aldo Moro 5, 00185 Rome (Italy)
francesca.pagnanelli@uniroma1.it

Secondary treatment of heavy metal bearing solutions requires highly expensive procedures including the application of ionic exchange resins or activated carbon packed in fixed bed reactors. The use of nanoparticles with magnetic properties as adsorbents can improve metal removal performances allowing for the achievement of high specific surface area. In addition, the simplification of the final solid-liquid separation by magnetic field can avoid the application of packed bed columns. In this study a simple synthetic pathway was optimized to produce copper nanoferrites ($CuFe_2O_4$), stable in water, magnetically active and with high specific area, to be further used as sorbent material for heavy metal removal in water solution. The hydrothermal route included surfactant-assisted coprecipitation (performed at different pH), hydrothermal treatment (1h at 120°C), washing with water and hexane, drying, and sintering (performed at 100 and 200°C for 1h). Structure and sizes of CuFe2O4 crystallites were studied as function of coprecipitation pH (8, 10, and 12.5) and sintering temperature (100-200°C). $CuFe_2O_4$ powders were characterized by field emission scanning electron microscopy (FE-SEM), energy dispersive X-ray spectroscopy (EDX), Brunauer-Emmett-Teller (BET) analysis of porosimetric data. Releasing tests of Fe and Cu at different pH were performed to define the pH range of stability in water. Potentiometric titrations were performed to determine the net charge depending on bulk solution pH. Best samples in terms of magnetic characteristics were obtained at pH 12.5 not depending on the sintering temperature. Mean size of nanoparticles obtained in such conditions was estimated by SEM images as 35-45 nm. BET analysis gave specific surface area of 147.8 ± 0.2 m2/g. CFNs have shown chemical stability in water solutions from pH 6 to 10. Zero charge point was estimated as pH 5.5. Then in the stability range of pH, CFNs present negative surface charge being able to coordinate positively charged heavy metal species.

1. Introduction

Magnetic nanoferrites with general structure MFe_2O_4 have been successfully synthesized through various methods. Most of ferrites can be obtained by hydrothermal synthesis with many advantages with respect to mechanochemical methods (Marinca et al., 2012; Šepelák et al., 2007) or thermolysis in organic solvents (Sarno et al.,2015).

In fact, hydrothermal synthesis enables to minimize time and energy consumption and is feasible for scale-up with the proven technology of pressure sealed reactors. Minimizing reaction time and reducing/eliminating sintering treatments is the new challenge aiming at further reduction of energy consumption. Furthermore, the direct precipitation of crystallized powders from solution ensures uniformity of nucleation, growth, and aging. Hydrothermal technique enhances the control of morphology and size of crystallites, reducing aggregation and determining a narrow particles distribution (Suchanek and Riman, 2006)

Hybrid hydrothermal syntheses are also widely used including synthesis assisted by capping agents /chelating agents /surfactants or additional treatments such as ultrasounds, microwaves and electric field application (Ortiz-Landeros et al.,2012).

In particular, the use of surfactants can enable the control of morphology and size of nanoparticles strictly depending on the specific chemical composition of the reaction medium.

Please cite this article as: Abo Atia T., Altimari P., Moscardini E., Pettiti I. , Toro L., Pagnanelli F., 2016, Synthesis and characterization of copper ferrite magnetic nanoparticles by hydrothermal route, Chemical Engineering Transactions, 47, 151-156 DOI: 10.3303/CET1647026

Most of the literature works reported the synthesis of pure copper ferrite nanoparticles with hydrothermal treatments at high temperatures (160-240°C) for long times (6-36 h), sometimes even followed by thermal treatment of sintering (500-1000°C).
As examples Zabihi et al., (2012) reported the synthesis of pure copper nanoferrites by 24 h hydrothermal route at 160°C with trisodium citrate as capping agent, and Salavati-Niasari et al., (2012) produced $CuFe_2O_4$ by coprecipitation at 80°C in presence of ottanoic acid, followed by 600°C sintering treatment. Other works also reported mild conditions of synthesis: Rashad et al., (2012) studied the formation of cubic copper ferrite at different hydrothermal temperature (100–200°C), treatment time (12–36 h), and pH conditions (8, 10, 12) without surfactant, showing the occurrence of Cu_2O and Fe_2O_3 only for intermediate values of pH.
Diodati et al., (2014) also performed hydrothermal low temperature route (76-135°C) for the synthesis of nanosized crystalline cobalt, nickel, zinc and manganese spinel ferrites starting from oxalate salts, showing the feasibility of such approach in the chosen conditions.
The main purpose of the present work was producing copper ferrite nanopowders minimizing energy consumption related both to hydrothermal treatment and final sintering of produced solids, but maximizing the amount of copper ferrite (usable as sorbent material) with respect to nonmagnetic and unstable copper and iron oxides. For such aim low temperature short time hydrothermal synthesis (1h at 120°C) was performed at different pH followed by sintering at two levels of low temperature (100 and 200°C). Best products obtained were further characterized about surface properties (surface net charge) in order to assess viability for heavy metal removal from aqueous solutions. Ferrites have been already used as absorbent materials for the removal of heavy metals in wastewater treatment. Srivastava et al., (2014) applied $MgFe_2O_4$ powders for cobalt recovery with efficient yields of removal, while Campos et al., (2010) and Malana et al.,(2011) functionalized magnetic ferrites nanoparticles with polymeric materials aiming at improving the removal of heavy metals.
The benefits of using magnetic nanopowders are inherent in the high surface-volume ratio and in the possibility of simplifying solid-liquid separation after heavy metal removal by applying magnetic fields.

2. Experimental

2.1 Materials

All the experiments were performed with analytical grade reagents: $CuSO_4$, $Fe_2(SO_4)_3 \cdot 5H_2O$ as precursors, DTAB (Dodecyiltrimethylammonium bromide) used as capping agent, NaOH as precipitation agent, hexane in washing treatment. HCl 0.1N and NaOH 0.1N standardized solutions have been used for surface charge determination.

2.2 Copper ferrites nanoparticles (CFNs) preparation

DTAB was dissolved in water under vigorous stirring in order to have a solution of 10^{-1} M corresponding to the lower boundary of CMC in water (Bahri et al., 2006). 1,596 g of copper (II) sulfate anhydrous and 4.90 g of iron (III) sulfate pentahydrate were added until complete dissolution in order to have Fe^{3+} 0.02 M and Cu^{2+} 0.01M, respecting copper ferrite molar ratio (Fe^{3+} /Cu^{2+} = 2). The precipitation pH was adjusted by NaOH 5M, in order to have 8, 10, 12.5 as final values. Aqueous solution was mixed for 45 minutes. The mixture was poured in autoclave vessels and kept at 120°C for 1 h. The black - brownish product was washed for two times with 50 ml of distilled water and was separated each time by centrifugation for 3 minutes at 3000 rpm. The final washing procedure was the same as before, but using 30 ml of hexane, instead of water. After solvent evaporation sintering at 100°C or 200°C for 24h was performed.
In table 1 the operating conditions used for the preparation of different samples of CNF were reported.

Table 1: Operating conditions for CNFs synthesis

Operating parameters	Sample A	Sample B	Sample C	Sample D	Sample E
pH	12.5	12.5	10	10	8
Sintering temperature(°C)	200	100	200	100	200

2.3 Characterization of CNFs

FE-SEM imaging and EDX analysis have been acquired by Zeiss Auriga FE-SEM. XRD patterns have been provided by Rigaku D-max. For nitrogen adsorption/desorption and BET surface area measurement a Micromeritics ASAP 2010 analyzer has been used. Surface area, (BET method) (Anderson and Pratt, 1985)

and textural analysis were obtained by N_2 adsorption/desorption measurement, at the liquid nitrogen temperature (-196 °C). The sample was pre-treated under vacuum at 180 °C for 2 hours. The pore distribution was determined by the BJH method (Barrett er al.1951) from the adsorption isotherm. The total pore volume was determined by the rule of Gurvitsch (Gurvitsch, 1915)
For the determination of the surface charge (q, meq/g) and the release of metals in solution, suspensions of 10 g/L of CNP were prepared. Final pH of CNP suspensions was changed by known volume addition of standard solutions of 1N HCl and 0.1 N NaOH. After 24 h shacking CFNs are separated, pH determined and the liquid analyzed with atomic absorption spectroscopy (AAS contrAA® 300 - Analytik Jena AG) to determine iron and copper concentrations.

3 Results and discussion

3.1 CNFs characterization

Samples A and B, obtained at pH 12.5, evidenced high homogeneity and uniformity of particle sizes with cubic-like structure of nanocrystals, typical for copper ferrites at low temperatures treatments, as confirmed in SEM images (Figure 1). SEM analyses indicated the formation of crystallites of 35-45 nm for both sample A and B. The effect of sintering temperature is not significant in the investigated range. In fact, lack of changes in the agglomeration of nanoparticles demonstrated a negligible effect of heat treatments between 100 and 200°C for samples A and B.
Samples A and B showed a precise arrangement of the microstructures, with a satisfactory repetition of copper ferrites clusters in the three dimensions, on the contrary C, D and E powders were, even at microscale, irregular and unorganized structures (Figure 2). These last structures can be assigned to clusters of copper oxides, whose presence was confirmed by XRD spectra (Figure 3). XRD patterns of samples A, B and C (Figure 3a) showed that the main phase of the powders was cuprospinel. Anyway another secondary phase, CuO (Tenorite) is present in different percentages in relationship to the different synthetic conditions. Semi-quantitative analysis obtained by XRD software (Match!2) revealed that decreasing pH from 12.5 (samples A and B) to 10 (sample C) determined an increased abundance of secondary phase CuO from 15-16% to 36%, respectively. The presence of CuO is then closely related to the pH of precipitation: at lower pH values, tenorite formation is favoured.
EDX analysis of produced samples revealed the presence of iron, copper, oxygen, carbon (traces of hexane and DTAB) and silicon (due to the specimen used for the analysis). In Figure 3b an example of EDX spectrum is reported for sample A. The relative abundance of elements in the different samples evaluated by EDX analyses confirmed the effect of pH on secondary phase formation. In fact, stoichiometric ratio 1:2 existing between Cu and Fe in $CuFe_2O_4$ is observed only at pH 12.5, while increasing relative amounts of Cu were observed in the other conditions as further prove of larger abundance of secondary tenorite phase in these cases.

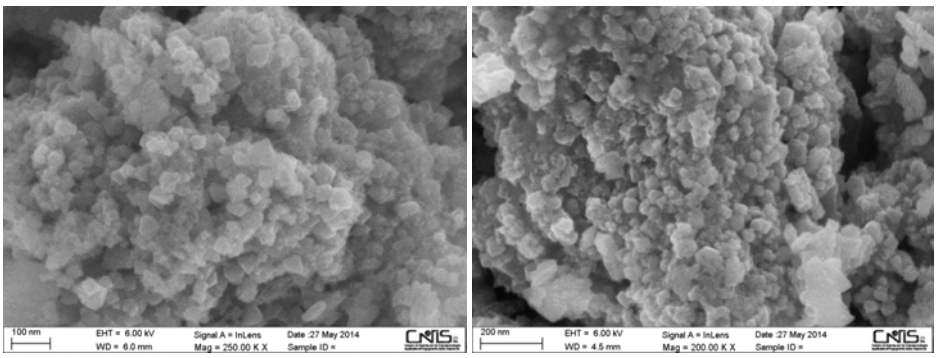

Figure 1: FE-SEM images of sample A -pH 12.5-200°C(left), sample B - pH 12.5-100°C(right)

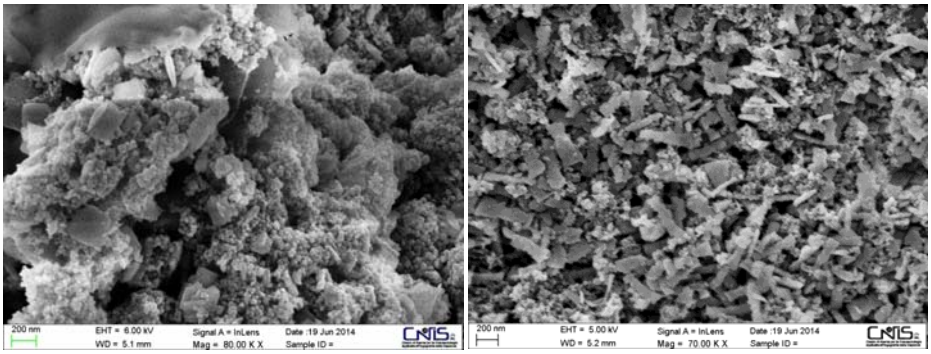

Figure2: FE-SEM images of sample C -pH 10-200°C(left), sample E - pH 8-200°C(right)

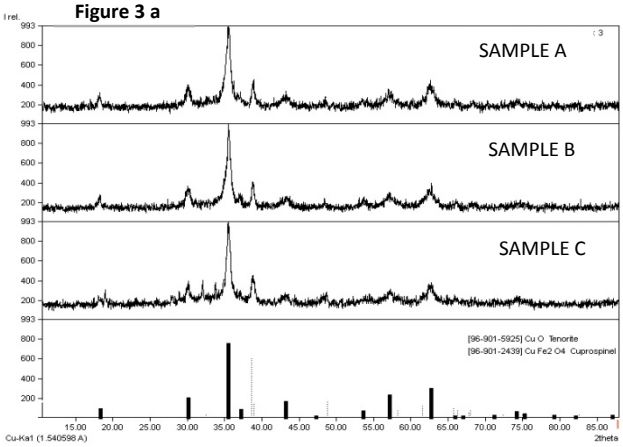

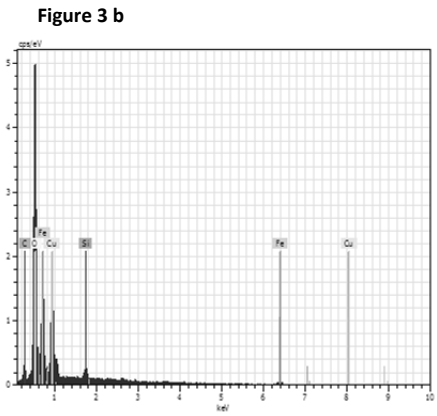

Figure 3 a) XRD patterns of sample A (pH 12.5-200°C), sample B (pH 12.5-100°C), sample C (pH 10-200°C) b) EDX analysis for sample A

Crystallite size for Sample A was estimated by XRD (using the full width at half maxima of peak 2theta=35.64 in the Scherer equation) (Cullity, 1978) as 19.8 nm. This result is in agreement with other reported in the literature for similar conditions, even if some differences can be observed. In particular, Rashad et al., (2012) obtained larger crystallite size (24.6 and 32.8 nm) for similar operating conditions: 150°C, pH 12 after 12 h and 36 h of treatment, respectively. Then a reduced size was obtained in the present work, which could be explained considering the addition of DTAB (limiting nanoparticle growth due to surface sorption), but also the effect of duration of hydrothermal treatment. In fact, increasing the time of hydrothermal treatment generally determined an increase of nanoparticle crystallite size (Rashad et al., 2012). Similarly, Diodati et al., (2014) found that hydrothermal treatment of 1 h gave lower crystallite size (25 nm for Mn and 10 nm for Ni) than using 24 h treatment (49 nm for Mn and 47 nm for Ni).
Also the effect of low temperature in hydrothermal phase can play in favour of reduced crystallite size as evidenced by Diodati et al., (2014): these authors found that for hydrothermal synthesis of Ni ferrites decreasing temperature from 135 to 100, and then to 75°C (for 24 h treatment) crystallite size passed from 47, 20, and 8 nm, respectively.
In view of these results short time and low temperature conditions in hydrothermal phase are conditions favouring reduction of both energy consumption and crystallite size.

3.2 Surface area and porosity

Sample A was investigated by nitrogen adsorption/desorption measurement as an example. The material revealed a mesoporous structure (isotherm type IV, hysteresis loop type H1, Figure 4) (Sing et al., 1985) with BET surface area of 148 m2g-1. According to the IUPAC classification, type H1 hysteresis loop is often associated with porous materials consisting of agglomerates in fairly regular array, and hence to have narrow distributions of pore size. From the desorption branch of the isotherm the pore size distribution was calculated

by the BJH method and gave a distribution of mesopores in the 2-10 nm range with a maximum at 3.8 nm. The total pore volume was 0.272 cm3g-1

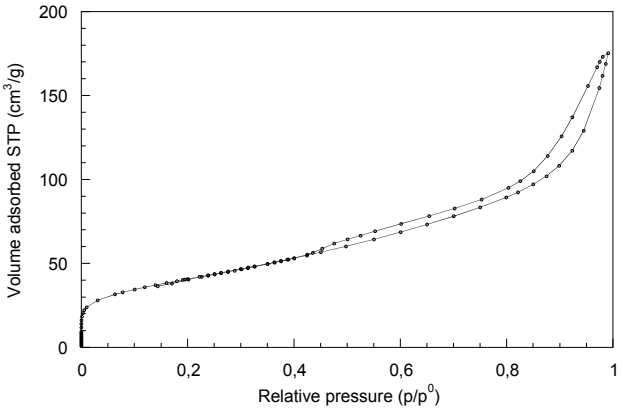

Figure 4: Adsorption/desorption isotherm of nitrogen at -196°C for sample A.

3.3 Metal release and surface charge

Release tests using samples A evidenced that for pH larger than 6 CFN are chemically stable in solution (Figure 5a). At lower pHs copper release was observed in water solution, probably due to the copresence of CuO.

Surface charge q (meq/g) determined by titration data using a condition of electroneutrality evidenced that CNF are characterized by positive net charge for pH lower than the pH of zero point charge (pH_{zpc}=5.5), while for larger pH values a negative net charge predominated.

Considering the pH range of chemical stability without metal release, CNFs could be used as sorbent for positively charged metallic species dissolved in solution.

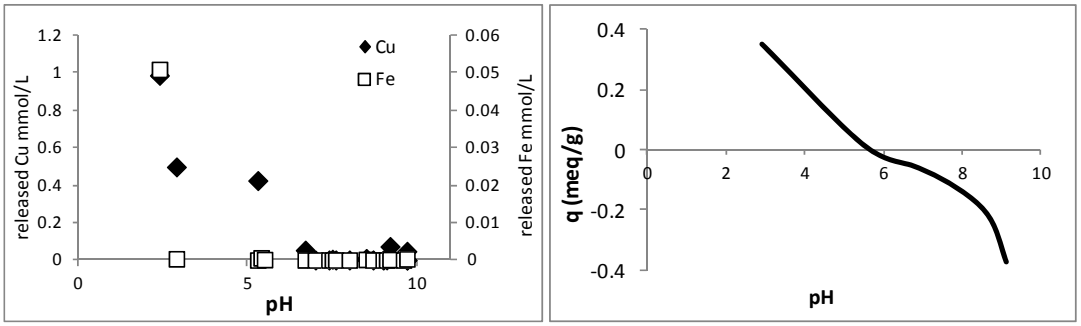

Figure 5: Leaching tests (left) and q vs pH (right) graphs for sample A. In q vs pH graph q (meq/g) is the surface charge at different pHs determined by titration with electroneutrality condition.

3. Conclusions

The synthetic route applied in this work comprehensive of DTAB-assisted coprecipitation, 1h hydrothermal treatment at 120°C, followed by low temperature heat treatment (100 °C) demonstrated to be a cheap and effective method for copper ferrites magnetic nanoparticle synthesis. Experimental findings denoted that pH of coprecipitation is determining the final amount of spinel magnetic phase: pH 12.5 giving the lowest amount of secondary CuO phase. At pH 12.5 the effect of sintering treatment was not significant in the investigated range (100- 200°C). In optimized conditions (pH 12.5, sintering temperature 100°C) copper ferrites nanoparticles of 35-45 nm were synthesized. SEM analysis confirmed the cubic ferrite spinel morphology, XRD patterns denoted that the powder main phase is cuprospinel, EDX that Cu/Fe molar ratio = 1:2, and BET analysis determined a specific surface area of 148 m^2g^{-1}. CFNs were tested in leaching tests showing a stability range for pH larger than 6, in which the particles exhibited a negative net charge (pH_{zpc}=5.5).

The experimental results reported in this work are promising in future applications aiming at reusing metals recovered from end of life hi tech wastes (such as batteries) (Moscardini et al., 2009) for the production of new sorbent materials to be used for the treatment of heavy metal bearing wastewaters. Further tests are now in course to investigate the sorbing capacity of these nanoparticles for metal removal from aqueous solution.

Acknowledgments

This research was co-funded from the European Community's Seventh Framework Programme (FP7/ 2007-2013) under grant agreement n°308549 (HydroWEEE Demo).

References

Anderson J.R., Pratt K.C., Eds., 1985. Introduction to Characterization and Testing of Catalysts, Academic Press, Australia.

Bahri M.A., Hoebeke M., Grammenos A., Delanaye L., Vandewalle N., Seret A., 2006, Investigation of SDS, DTAB and CTAB micelle microviscosities by electron spin resonance, Colloids and Surfaces A: Physicochemical and Engineering Aspects, 290, 206-212.

Barrett E.P., Joyner L.G., Halenda P.P., 1951. The Determination of Pore Volume and Area Distributions in Porous Substances. I. Computations from Nitrogen Isotherms J. Am. Ceram. Soc. 73, 373-380.

Cullity B.D., 1978, Elements of X-ray diffraction. Addison-Wesley, Reading.

Campos A.F.C., Ferreira M.A., Marinho E.P., Tourinho F.A., Depeyrot J., 2010, Synthesis and design of functionalized magnetic nanocolloids for water pollution remediation, Physics Procedia, 9, 45-48.

Diodati S., Pandolfo L., Caneschi A., Gialanella S., Gross S., 2014, Green and low temperature synthesis of nanocrystalline transition metal ferrites by simple wet chemistry routes, Nano Research, 7(7), 1027–1042.

Gurvitsch L., 1915, Physicochemical Attractive Force, J. Phys. Chem. Soc. Russ. 47, 805-827.

Malana M.A., Qureshi R.B., Ashiq M.N., 2011, Adsorption studies of arsenic on nano aluminium doped manganese copper ferrite polymer (MA, VA, AA) composite: Kinetics and mechanism, Chemical Engineering Journal, 172, 721-727.

Marinca T.F., Chicinas I., Isnard O., 2012, Influence of the heat treatment conditions on the formation of CuFe2O4 from mechanical milled precursors oxides, J. Therm. Anal. Calorim., 110, 301–307.

Moscardini E., Furlani G., Pagnanelli F., Ferella F., De Michelis I., Vegliò F., Beolchini F., Toro L.,2009 Process for the treatment of alkaline spent batteries. Chemical Engineering Transactions Vol. 17, 281-286.

Ortiz-Landeros J., Gómez-Yáñez C., López-Jureáz R., Dávalos-Velasco I., Pfeiffer H., 2012, Synthesis of advanced ceramics by hydrothermal crystallization and modified related methods, Journal of Advanced Ceramics 1(3), 204-220.

Salavati-Niasari M., Mahmoudi T., Sabet M., Hosseinpour-Mashkani S.M., Soofivand F., Tavakoli F., 2012, Synthesis and Characterization of Copper Ferrite Nanocrystals via Coprecipitation, J. Clust. Sci., 23, 1003–1010.

Sarno M., Cirillo C., Ponticorvo E., Ciambelli P., 2015, Synthesis and characterization of flg/fe3o4 nanohybrid supercapacitor, Chemical Engineering Transactions, 43, 727-732.

Šepelák V., Bergmann I., Feldhoff A., Heitjans P., Krumeich F., Menzel D., Litterst F.J., Campbell S.J., Becker K.D., 2007, Nanocrystalline Nickel Ferrite, NiFe2O4: Mechanosynthesis, Nonequilibrium Cation Distribution, Canted Spin Arrangement, and Magnetic Behavior, J. Phys. Chem. C, 111(13), 5026–5033.

Sing K.S.W., Everett D.H., Haul R.A.W., Moscou L., Pierotti R.A., Rouquerol J., Siemieniewska T., 1985, Reporting physisorption data for gas/solid systems with special reference to the determination of surface area and porosity, Pure Appl. Chem. 57, 603-619

Srivastava V., Sharma Y.C., Sillanpää M., 2015, Application of nano-magnesso ferrite (n-MgFe2O4) for the removal of Co2+ ions from synthetic wastewater: Kinetic, equilibrium and thermodynamic studies, Applied Surface Science, 338, 42-54

Suchanek W.L., Riman R.E., 2006, Hydrothermal Synthesis of Advanced Ceramic Powders, Advances in Science and Technology, 45, 184-193.

Rashad M.M., Mohamed R.M., Ibrahim M.A., Ismail L.F.M., Abdel-Aal E.A., 2012, Magnetic and catalytic properties of cubic copper ferrite nanopowders synthesized from secondary resources, Advanced Powder Technology, 23, 315-323.

Zabihi F., Isfahani T.D., Hadi I., 2012, Hydrothermal synthesis of copper ferrite nanoparticles by sodium citrate synthetic process, Proceedings of the 4th International Conference on Nanostructures (ICNS4) 1394-1396, 12-14 March, 2012, Kish Island, I.R. Iran.